Supplementary information

"QuaNCAT: quantitating proteome dynamics in primary cells"

by Andrew J. M. Howden, et al. *Nature Method,* 2013

Content:

1. Supplementary Figures 1-6.
2. Supplementary Table 2
3. Supplementary Note: Chemical synthesis description and other methods used to acquire data for Supplementary Figures.

Supplementary Figure 1

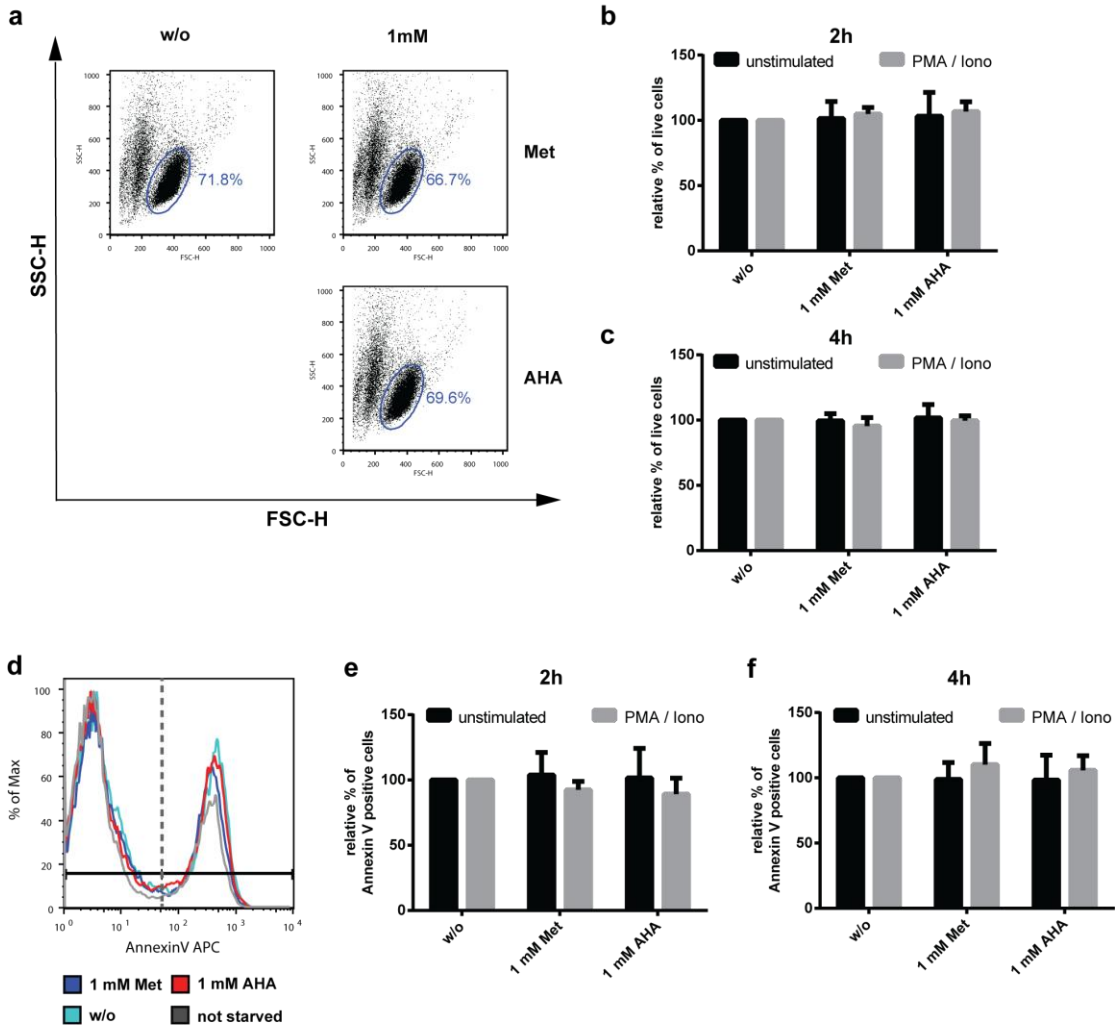

Supplementary Figure 1. Effect of azidohomalanine on cell morphology and viability in non-stimulated and stimulated primary human T-lymphocytes. Human primary CD4+ T-lymphocytes were starved in Met-, Arg- and Lys-free RPMI for 1 h followed by incubation for 2- or 4 h in RPMI supplemented with 'heavy' Arg ($^{13}C_6$,$^{15}N_4$-L-Arg) and Lys ($^{13}C_6$,$^{15}N_2$-L-Lys) and 1 mM of AHA or Met. Cells pulsed with 'heavy' Arg and Lys but without (w/o) Met served as controls. In addition, cells were either left non-stimulated or stimulated with PMA at 62.5 ng/ml and Ionomycin (Iono) at 1 µg/ml. (**a – c**) Cell morphology was assessed by flow cytometry. FSC/SSC dot plots (cell size/cell granularity) were used to determine cell viability. (**a**) Representative FSC/SSC dot plots after the 4 h pulse with 1 mM Met and AHA plus PMA/Ionomycin stimulation. Diagrams represent the mean percentage of live cells of six independent blood donors after 2 h (**b**) and 4 h (**c**), normalized to w/o-Met treated cells. Error bars, s.d. (*n*=6). (**d-f**) Quantitation of apoptotic cells was obtained using

flow cytometry by monitoring cell surface expression of phosphatidylserine by Annexin V. (**d**) Representative histogram of Annexin V staining after 4 h pulse with 1 mM Met and AHA plus PMA/Ionomycin stimulation. Diagrams represent the mean percentage of Annexin V positive cells after 2 h (**e**) and 4 h (**f**) normalized to w/o L-Met treated cells. Error bars, s.d. (*n*=6). Statistical analysis (two-way analysis of variance (ANOVA) followed by Tukey's multiple comparison test) revealed no significant changes between all conditions tested. Neither 1 mM, 4 mM AHA (data not shown) nor long-term treatment (4 h) affected viability of human primary T-cells.

Supplementary Figure 2

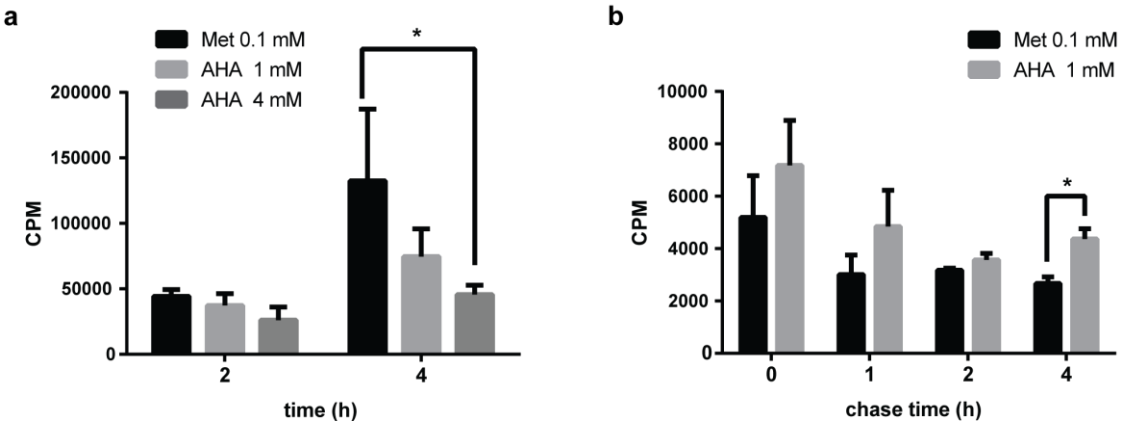

Supplementary Figure 2. Effect of azidohomoalanine on global protein synthesis and degradation. (**a**) Protein synthesis. After 1 h L-methionine (Met) and L-cysteine (Cys) starvation, Jurkat T cells were incubated with RPMI supplemented with 0.1 mM Met, 1 mM or 4 mM azidohomoalanine (AHA). 10 nM (10 µCi/ml) ^{35}S-Cys plus 5 µM L-Cys were then added to both media. After a pulse of 2 and 4 h, samples were harvested and lysed. Soluble proteins were precipitated with 5% Trichloroacetic acid, spotted on filter paper and air-dried. Spots were excised and radioactivity was measured with a scintillation counter. The diagram represents the mean counts per minute (CPM) from one experiment performed in triplicate. Error bars, s.d. (*n*=3), (*) *P*<0.05. (**b**) Protein degradation. After 1 h L-methionine (Met) and L-cysteine (Cys) starvation, Jurkat T cells were incubated with RPMI supplemented with either 0.1 mM Met or 1 mM azidohomoalanine (AHA). 32.4 nM (30 µCi/ml) ^{35}S-Cys plus 16.2 µM L-Cys were then added to both media. After a pulse of 15 minutes, media were replaced with fresh, Met (0.1 mM) or AHA (1 mM) containing media lacking radioactive Cys. After 0, 1, 2 and 4 h, cells were harvested and lysed. Soluble proteins were prepared as described in (a) and radioactivity measured with a scintillation counter. The diagram shows the mean counts per minute (CPM) representative for two independent experiments performed in triplicate. Error bars, s.d. (*n*=3), (*) *P*<0.05. Statistical analysis (one-way analysis of variance (ANOVA) followed by Bonferroni's multiple comparison test) revealed a significant decrease in global protein synthesis (a) after 4 h of 4 mM AHA treatment compared to Met. Collectively, these data show that AHA, at a concentration of 4 mM has a time-dependent effect on protein biosynthesis compared to AHA at 1 mM. We therefore proceeded with a concentration of 1 mM and examined the influence of AHA on global protein degradation in a ^{35}S-Cysteine pulse-chase experiment (b). Statistical

analysis (unpaired t-test) revealed significant changes in protein degradation for AHA-treated relative to Methionine-treated cells only after 4 h.

Supplementary Figure 3

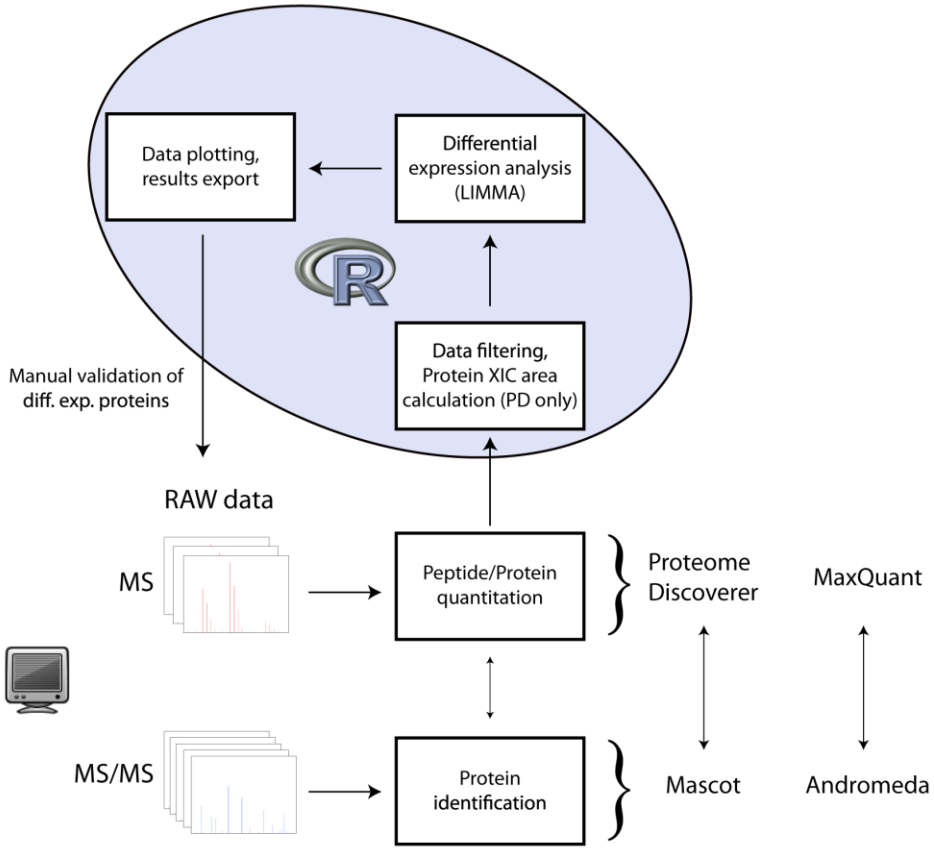

Supplementary Figure 3. Workflow of MS data processing, search and analysis. Raw MS data were processed by Proteome Discoverer 1.3 (PD) and MaxQuant 1.3.0.5 (MQ). Database searches were performed using Mascot (PD) or Andromeda (MQ). Data were imported into R and protein extracted ion chromatogram (XIC) areas were calculated in the case of PD. Proteins that were reproducibly quantified (see online methods) were submitted for differential expression analysis using LIMMA. The resulting information was then used to generate various diagnostic plots (e.g. Volcano plots) and produce a list of differentially expressed proteins. Quantitation for these proteins was then manually validated through inspection of the raw data. The manual validation involved verifying that the top three (when applicable) most abundant SILAC pairs, used by PD or MQ for quantitating each protein, supported the change in expression indicated by the software packages.

Supplementary Figure 4

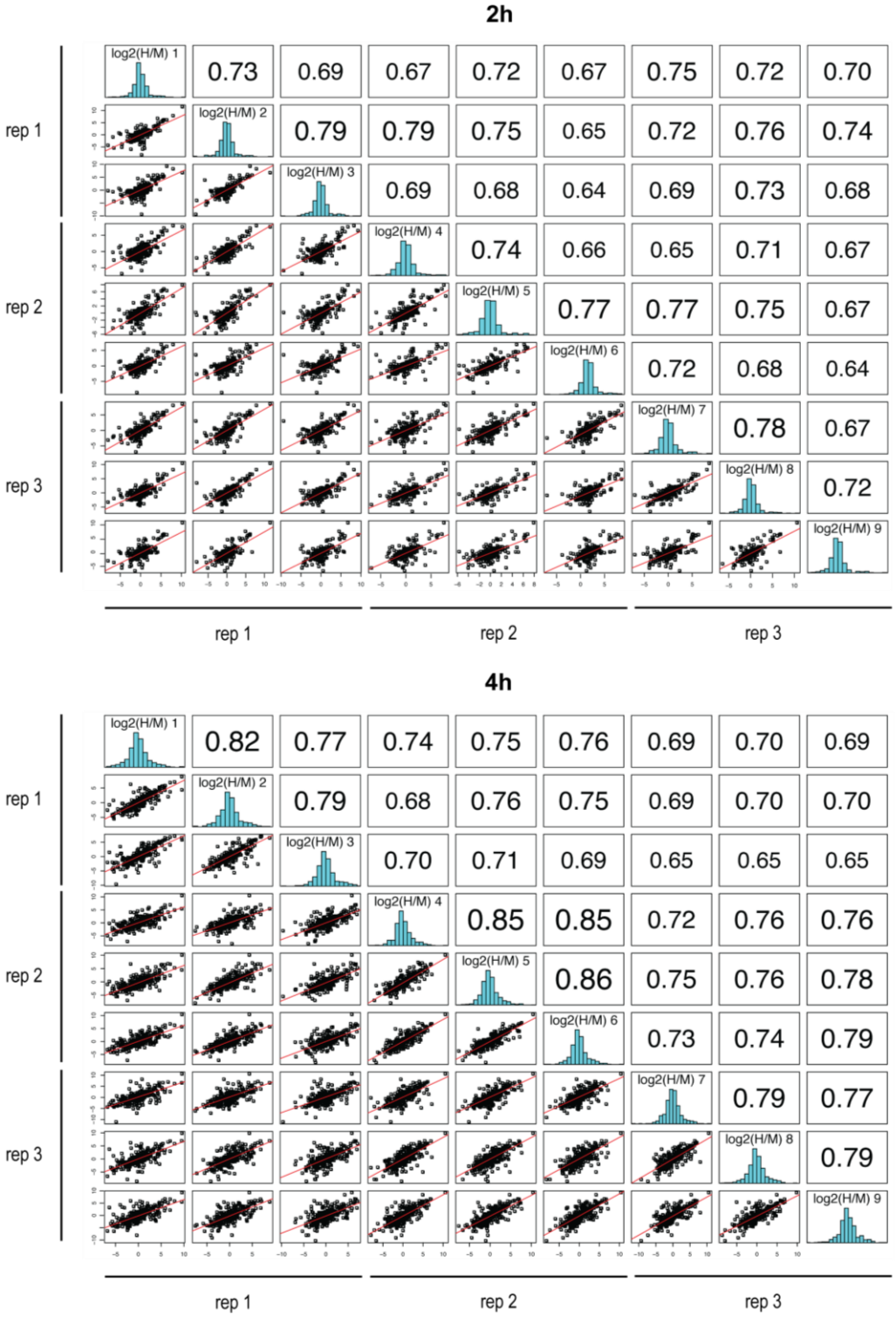

Supplementary Figure 4. Reproducibility of protein log_2 H/M ratios between nanoLC-MS/MS runs for all replicas. Scatterplots of protein log_2 H/M ratios for nanoLC-MS/MS run pairs and corresponding Pearson correlation coefficients for 2

and 4 h treatments. Linear regression lines are shown in red. Histograms of protein $\log_2$ H/M ratios for each run are plotted across the matrix diagonal. Global average Pearson correlation coefficients were 0.71 (0.64-0.79) and 0.74 (0.65-0.86) for 2 h and 4 h stimulation, respectively, indicating a good reproducibility of the QuaNCAT procedure.

Supplementary Figure 5

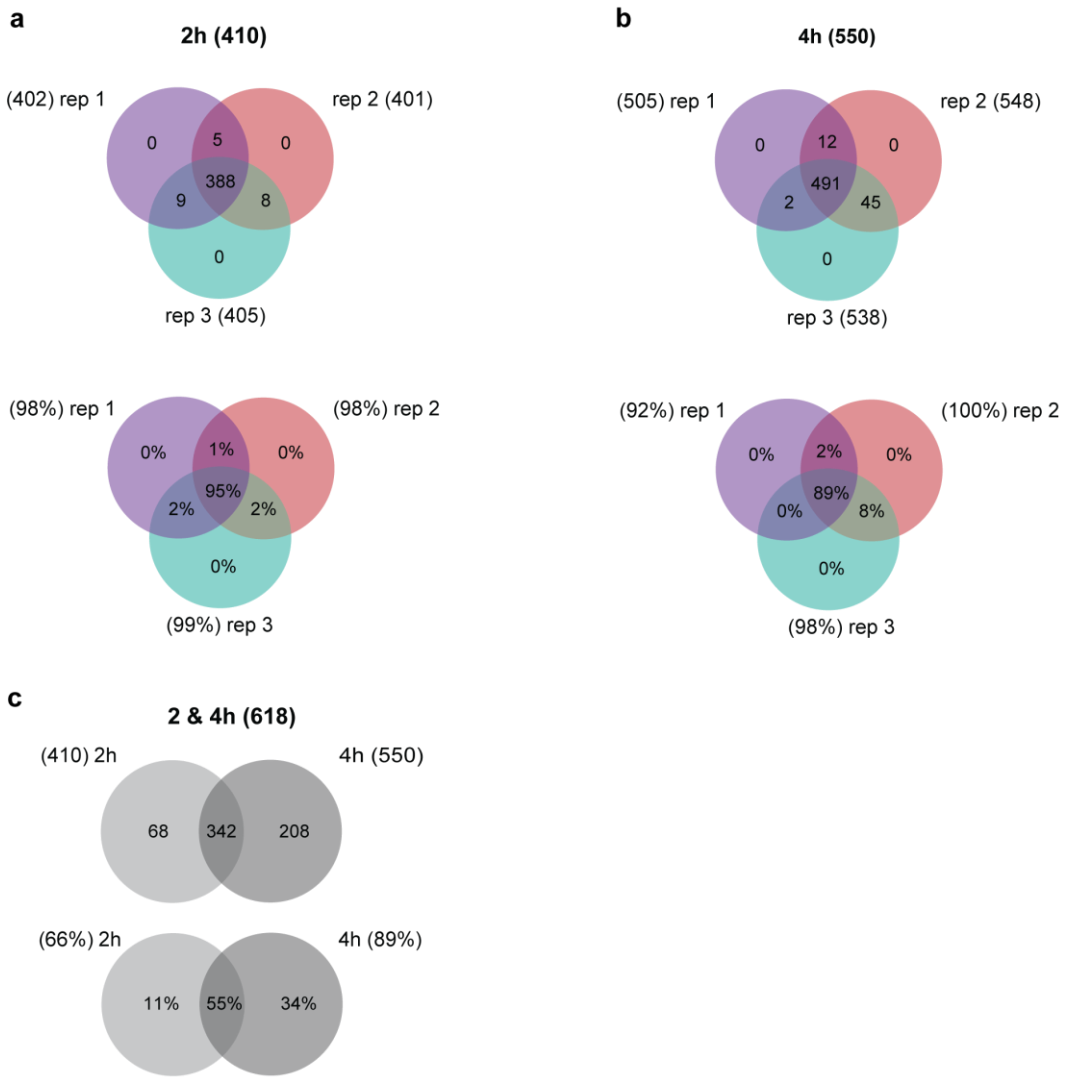

Supplementary Figure 5. Reproducibility of quantified protein subset submitted for differential expression analysis using LIMMA. (**a**) Venn diagrams showing the overlap in number (top) and percentage (bottom) of quantified proteins, respectively, between replicates for the 2 h data. (**b**) Respective Venn diagrams for the 4 h data. (**c**) Venn diagrams showing the overlap in Protein IDs between the 2 and 4 h data.

Supplementary Figure 6

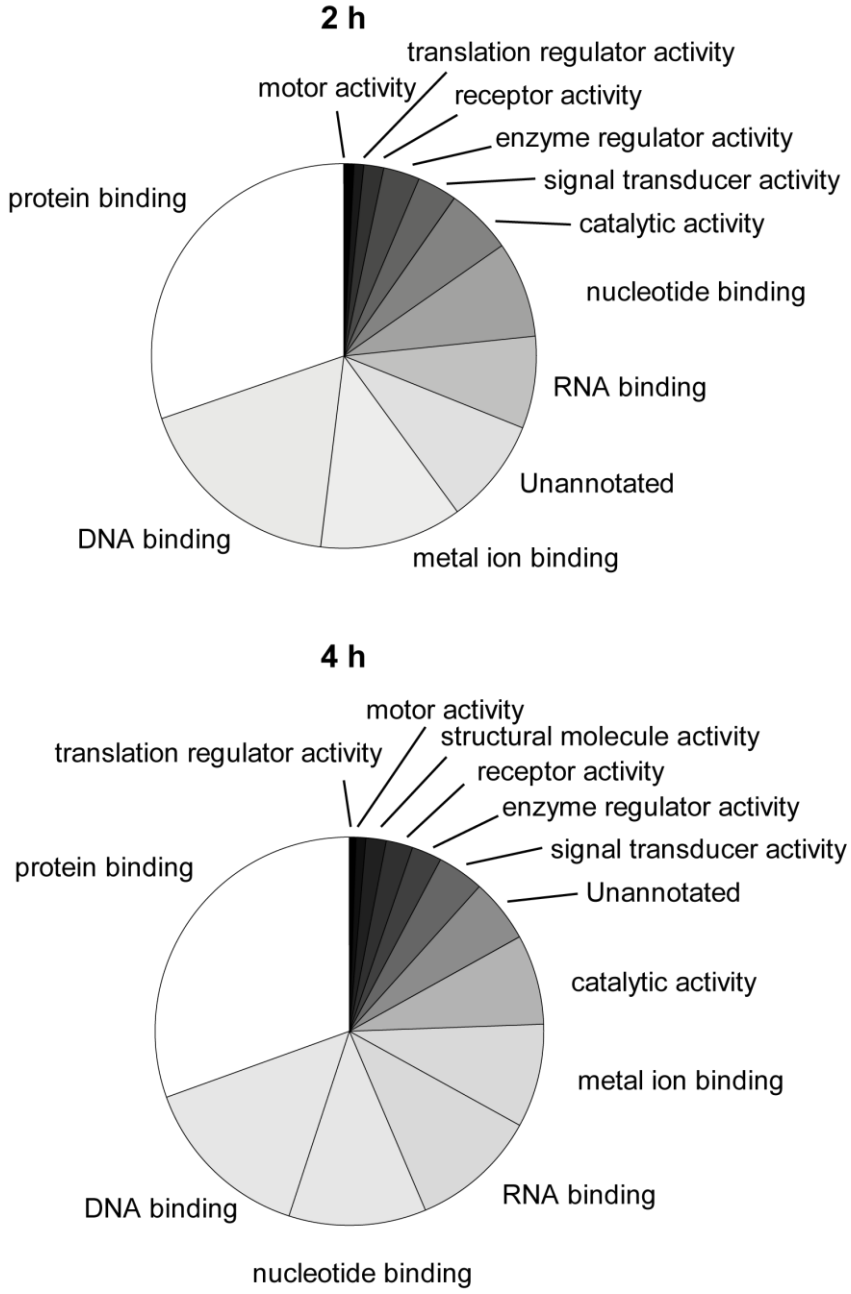

Supplementary Figure 6. **Breakdown of differentially expressed proteins according to molecular function.** Differentially expressed proteins at 2 and 4 h of stimulation were uploaded to Protein Center and annotated according to Gene Ontology terms.

Supplementary Table 2

	Uniprot Accession	Gene Symbol	Protein description	2h fold-change (H vs M)	4h fold-change (H vs M)	Fold change (4 vs 2h)	MaxQuant only
1	P01100	FOS	Proto-oncogene c-Fos	589.3	510.5	-1.154	
2	P04141	CSF2	Granulocyte-macrophage colony-stimulating factor		118.5		
3	P53539	FOSB	Protein fosB	182.4	48.0	-3.802	
4	P11161-2	EGR2	Isoform Short of E3 SUMO-protein ligase EGR2	101.9	101.0	-1.009	
5	Q03060-11	CREM	Isoform 9 of cAMP-responsive element modulator		93.8		
6	P18146	EGR1	Early growth response protein 1	47.9	79.7	1.665	
7	Q9BYH8	NFKBIZ	NF-kappa-B inhibitor zeta	72.9	50.6	-1.439	
8	Q6NXU0	NR4A2	Nuclear receptor subfamily 4 group A member 2	58.4	58.8	1.007	
9	Q92570-3	NR4A3	Isoform 3 of Nuclear receptor subfamily 4 group A member 3		39.4		
10	O00560	SDCBP	Syntenin-1	37.7	34.5	-1.094	
11	Q702N8	XIRP1	Xin actin-binding repeat-containing protein 1		36.0		
12	P01579	IFNG	Interferon gamma		30.0		
13	P15408	FOSL2	Fos-related antigen 2		29.7		
14	Q8N103	TAGAP	T-cell activation Rho GTPase-activating protein	25.0			
15	P17275	JUNB	Transcription factor jun-B	24.5	25.0	1.021	
16	Q17RU2	REL	Proto-oncogene c-Rel		22.7		
17	P26651	ZFP36	Tristetraprolin	22.2			
18	Q2M1K9	ZNF423	Zinc finger protein 423	21.7			+
19	Q15596	NCOA2	Nuclear receptor coactivator 2		20.1		
20	Q96QC0	PPP1R10	Serine/threonine-protein phosphatase 1 regulatory subunit 10	25.8	12.2	-2.113	
21	F2Z3D5	IRF4	Interferon regulatory factor 4	18.8	18.7	-1.005	
22	Q5D1E8	ZC3H12A	Ribonuclease ZC3H12A	15.3	19.1	1.253	
23	O15523	DDX3Y	ATP-dependent RNA helicase DDX3Y		16.4		
24	Q06889	EGR3	Early growth response protein 3		17.9		+
25	Q07108	CD69	Early activation antigen CD69		15.7		
26	P38159	RBMX	RNA-binding motif protein, X chromosome		13.0		
27	P11387	TOP1	DNA topoisomerase 1		11.6		
28	O75157-2	TSC22D2	Isoform 2 of TSC22 domain family protein 2	17.0	6.1	-2.767	
29	Q7Z417	NUFIP2	Nuclear fragile X mental retardation-interacting protein 2		11.4		
30	P08238	HSP90AB1	Heat shock protein HSP 90-beta		11.1		
31	A6NE42	TGIF1	Homeobox protein TGIF1	6.8	14.0	2.050	
32	P32456	GBP2	Interferon-induced guanylate-binding protein 2		10.1		
33	P10914	IRF1	Interferon regulatory factor 1		10.0		
34	O15054-1	KDM6B	Lysine-specific demethylase 6B	13.2	6.1	-2.171	+
35	P38936	CDKN1A	Cyclin-dependent kinase inhibitor 1	8.3			+
36	P11940	PABPC1	Polyadenylate-binding protein 1	6.4	9.6	1.509	
37	Q9Y3B9	RRP15	RRP15-like protein		7.9		
38	O00571	DDX3X	ATP-dependent RNA helicase DDX3X	7.4			
39	Q9NTZ6	RBM12	RNA-binding protein 12		7.3		
40	Q99622	C12orf57	Protein C10	3.2	9.5	2.965	
41	Q07352	ZFP36L1	Zinc finger protein 36, C3H1 type-like 1	4.9	7.5	1.518	
42	P13693	TPT1	Translationally-controlled tumor protein		6.1		
43	Q92598-2	HSPH1	Isoform Beta of Heat shock protein 105 kDa		5.8		
44	Q13118	KLF10	Krueppel-like factor 10	5.7			+
45	P55040	GEM	GTP-binding protein GEM		5.4		+
46	Q9BYV9	BACH2	Transcription regulator protein BACH2		5.5		+
47	P60842	EIF4A1	Eukaryotic initiation factor 4A-I	1.6	9.4	5.742	
48	P05412	JUN	Transcription factor AP-1	5.3			
49	P31689	DNAJA1	DnaJ homolog subfamily A member 1	4.7			
50	Q7LC44	ARC	Activity-regulated cytoskeleton-associated protein		4.6		+
51	Q9NYJ8	TAB2	TGF-beta-activated kinase 1 and MAP3K7-binding protein 2		4.3		
52	P18847	ATF3	Cyclic AMP-dependent transcription factor ATF-3		4.4		+
53	P16070-16	CD44	Isoform 16 of CD44 antigen		4.1		
54	O94992	HEXIM1	Protein HEXIM1		4.0		
55	F6RU81	C14orf43	Uncharacterized protein C14orf43 (Fragment)	4.0			
56	O95817	BAG3	BAG family molecular chaperone regulator 3	3.6			
57	Q9ULX9	MAFF	Transcription factor MafF	3.3	3.9	1.174	
58	Q8WWM7	ATXN2L	Ataxin-2-like protein	3.6			
59	Q9H334	FOXP1	Forkhead box protein P1		3.5		+
60	P17844	DDX5	Probable ATP-dependent RNA helicase DDX5	3.0	3.9	1.327	
61	Q7L1Q6-3	BZW1	Basic leucine zipper and W2 domain-containing protein 1		3.4		+
62	Q9UKI2	CDC42EP3	Cdc42 effector protein 3		3.1		+
63	P62857	RPS28	40S ribosomal protein S28		3.1		
64	P08670	VIM	Vimentin		3.0		
65	P48960	CD97	CD97 antigen		3.0		+
66	P17535	JUND	Transcription factor jun-D	2.9			+
67	P18583-9	SON	Protein SON		2.8		+
68	P10124	SRGN	Serglycin	2.2	3.3	1.504	
69	P68104	EEF1A1	Elongation factor 1-alpha 1		2.7		
70	P23246	SFPQ	Splicing factor, proline- and glutamine-rich	2.6	2.8	1.063	
71	P20290	BTF3	Transcription factor BTF3		2.6		+
72	P15311	EZR	Ezrin	1.9	3.2	1.730	
73	Q92804	TAF15	TATA-binding protein-associated factor 2N	6.4	2.5	-2.591	+
74	H0YI46	CHMP4A	Charged multivesicular body protein 4a (Fragment)	2.4			
75	P30443	HLA-A	HLA class I histocompatibility antigen, A-3 alpha chain	2.4			
76	P67809	YBX1	Nuclease-sensitive element-binding protein 1		2.4		+
77	Q8WVC2	RPS21	40S ribosomal protein S21		2.3		
78	O94842	TOX4	TOX high mobility group box family member 4		2.3		+
79	O76080	ZFAND5	AN1-type zinc finger protein 5		2.3		+
80	P23588	EIF4B	Eukaryotic translation initiation factor 4B		2.2		
81	Q9Y244	POMP	Proteasome maturation protein	2.2			+
82	Q53QV2	LBH	Protein LBH		2.1		
83	Q7LBR1	CHMP1B	Charged multivesicular body protein 1b	2.1			
84	Q9Y520-4	PRRC2C	Isoform 4 of Protein PRRC2C	1.8	2.1	1.157	
85	B7Z4V2	HSPA9	Stress-70 protein, mitochondrial	1.9	2.2	1.201	
86	P98179	RBM3	Putative RNA-binding protein 3		2.0		
87	P31943	HNRNPH1	Heterogeneous nuclear ribonucleoprotein H		2.0		
88	F8VXY0	HNRNPA1	Heterogeneous nuclear ribonucleoprotein A1		1.9		
89	P11021	HSPA5	78 kDa glucose-regulated protein		1.8		
90	A8MWD9	SNRPG	Small nuclear ribonucleoprotein G-like protein		1.8		
91	Q9UQ35	SRRM2	Serine/arginine repetitive matrix protein 2	1.7	1.9	1.104	
92	Q96K17	BTF3L4	Transcription factor BTF3 homolog 4	1.6			
93	H0Y7A7	CALM2	Calmodulin	1.7			+
94	E9PEC0	ADRM1	Proteasomal ubiquitin receptor ADRM1	-1.7			
95	Q9H3Y8	PPDPF	Pancreatic progenitor cell differentiation and proliferation factor	-2.5			+
96	O00161	SNAP23	Synaptosomal-associated protein 23		-2.6		
97	Q9Y2Y9	KLF13	Krueppel-like factor 13	-2.8			
98	B4DLJ8	HLA-DRA	HLA class II histocompatibility antigen, DR alpha chain	-3.2			
99	P13501	CCL5	C-C motif chemokine 5		-3.8		
100	F5GZU5	MED15	Mediator of RNA polymerase II transcription subunit 15		-4.0		
101	Q86UU0-4	BCL9L	Isoform 4 of B-cell CLL/lymphoma 9-like protein	-1.8	-6.9	3.751	
102	P33241	LSP1	Lymphocyte-specific protein 1	-2.9	-4.5	1.556	
103	P06702	S100A9	Protein S100-A9	-3.1	-5.4	1.724	
104	P17931	LGALS3	Galectin-3	-5.7	-7.3	1.288	
105	Q9P2R6	RERE	Arginine-glutamic acid dipeptide repeats protein	-8.3			+
106	Q15025-2	TNIP1	Isoform 2 of TNFAIP3-interacting protein 1	-4.8	-12.3	2.588	
107	P28799	GRN	Granulins	-5.9	-15.6	2.658	

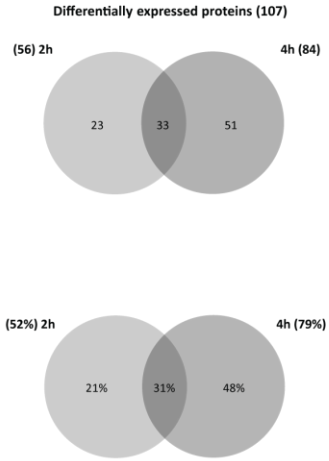

Supplementary Table 2. List of differentially expressed proteins after 2 and 4 h of PMA/Ionomycin primary T cell stimulation that was manually validated after statistical analysis using LIMMA. On the right are Venn diagrams showing the overlap of

protein IDs between the two time points as absolute numbers and percentages of the total number of identified proteins.

General experimental procedures for chemical synthesis

Melting points (m.p.) were recorded on a Leica Galen III hot stage microscope equipped with a Testo 720 thermocouple probe and are uncorrected. Proton nuclear magnetic resonance (^{1}H NMR) spectra were recorded on a Bruker AVII500 (500 MHz) or on a Bruker DQX400 (400 MHz) spectrometer, as indicated. Carbon nuclear magnetic resonance (^{13}C NMR) spectra were recorded on a Bruker AVII500 (125 MHz) or on a Bruker DQX400 (100 MHz) spectrometer, as indicated. NMR Spectra were fully assigned using COSY, HSQC, HMBC, and NOESY. All chemical shifts are quoted on the δ scale in ppm using residual solvent as the internal standard (^{1}H NMR: $CDCl_3$ = 7.26, CD_3OD = 4.87; DMSO-d_6 = 2.50 and ^{13}C NMR: $CDCl_3$ = 77.0; CD_3OD = 49.0; DMSO-d_6 = 39.5). Coupling constants (J) are reported in Hz with the following splitting abbreviations: s = singlet, d = doublet, t = triplet, q = quartet, quin = quintet, and a = apparent.

Infrared (IR) spectra were recorded on a Bruker Tensor 27 Fourier Transform spectrophotometer using thin films on NaCl plates for liquids and oils and KBr discs for solids and crystals. Absorption maxima (υ_{max}) are reported in wavenumbers (cm^{-1}). For compound characterization low resolution mass spectra (LRMS) were recorded on a Waters Micromass LCT Premier TOF spectrometer using electrospray ionization (ESI) and high resolution mass spectra (HRMS) were recorded on a Bruker MicroTOF ESI mass spectrometer. Nominal and exact *m/z* values are reported in Daltons. Optical rotations were measured on a Perkin–Elmer 241 polarimeter with a path length of 1.0 dm and are reported with implied units of 10^{-1} deg cm^2 g^{-1}. Concentrations (c) are given in g/100 ml. Thin layer chromatography (TLC) was carried out using Merck aluminium backed sheets coated with 60F254 silica gel. Visualization of the silica plates was achieved using a UV lamp (λ_{max} = 254 nm), and/or ammonium molybdate (5 % in 2 M H_2SO_4), and/or potassium permanganate (5 % $KMnO_4$ in 1 M NaOH with 5 % potassium carbonate). Flash column chromatography was carried out using BDH 40–63 μm silica gel (VWR). Mobile phases are reported in relative composition (*e.g.* 1:2:4 H_2O/*i*PrOH/EtOAc). Anhydrous solvents were purchased from Fluka or Acros. Triethylamine was stored over NaOH pellets. All other solvents were used as supplied (Analytical or HPLC grade), without prior purification. Distilled water was used for chemical reactions and Milli–QR purified water for protein manipulations. Reagents were purchased from Aldrich and used as supplied, unless otherwise indicated. 'Petrol' refers to the

fraction of light petroleum ether boiling in the range 40–60 ºC. All reactions using anhydrous conditions were performed using flame-dried apparatus under an atmosphere of argon or nitrogen. Brine refers to a saturated solution of sodium chloride. Anhydrous magnesium sulfate ($MgSO_4$) was used as drying agents after reaction workup, as indicated. DOWEX 50WX8 (H^+ form) was conditioned as follows: 100 g of the commercial resin was placed in a 500 mL sintered filter funnel and allowed to swell with 200 mL of acetone for 5 minutes. The solvent was removed by suction and the resin was washed successively with 800 mL of acetone, 500 mL methanol, 500 mL 5 M HCl, and then 1 L of water or until the pH of filtrate was ~ 7, as indicated by pH paper. The resin was partially dried on the filter and then stored and used as needed.

Synthesis of Azidohomoalanine

L-azidohomoalanine was prepared using a method adapted from the literature as follows.[25]

Step 1: Hofmann degradation of *N*-tert-butoxycarbonyl-(*S*)-glutamine:

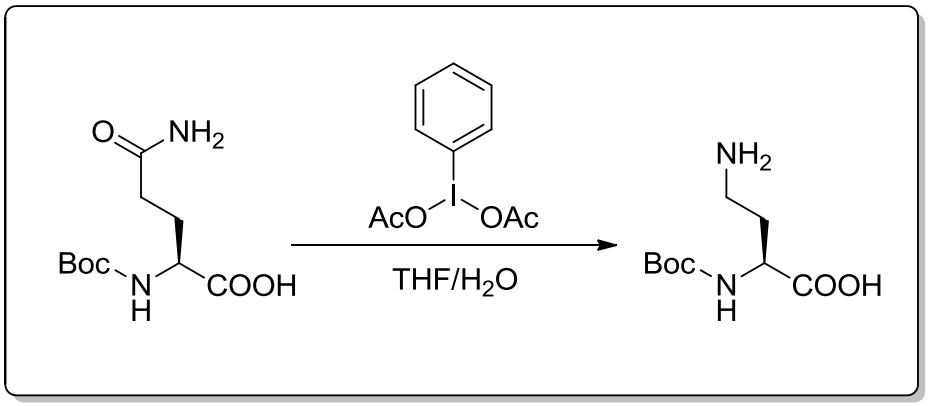

N-tert-Butoxycarbonyl-(*S*)-glutamine (5.0 g, 20.3 mmol) was dissolved in THF (48 mL) and water (12 mL). The solution was cooled in an ice bath, and (Diacetoxyiodo)benzene (7.8 g, 24.2 mmol) was added. The reaction was monitored by TLC (4:1:1 n-butanol: acetic Acid: water). After 6 hours, the organic portion was evaporated in vacuo. The aqueous portion was diluted with water, and extracted with ethyl acetate (3 x 30 mL). The aqueous portion was then partially evaporated, frozen, and lyophilised. The product was obtained as a solid (3.1 g, 71 %). IR (ν_{max}, film): 3416, 2977, 2931, 1698, 1589, 1561, 1529, 1499, 1439, 1392, 1366, 1252, 1161, 1052, 1029, 949, 907, 868, 802. ^{1}H NMR (400 MHz, D_2O) δ: 3.86 (m, 1H, C*H*), 2.94 (t, *J* = 7.8 Hz, 2H, NH_2CH_2), 1.9 (m, 1H, CH_2), 1.85 (m, 1H, CH_2), 1.31 (s, 9H,

C(C*H*$_3$)$_3$). LRMS (ESI) Calculated: [M-H] $C_9H_{18}N_2O_4$ (m/z): 218, Obtained: $[M-H]^-$: 217.12, $[2M-H]^-$: 435.26, $[M+H]^+$: 219.16

Step 2: Conversion of unprotected amine to azide using triflic azide. Triflic azide was prepared in situ, and the reaction was adapted from literature.[26]

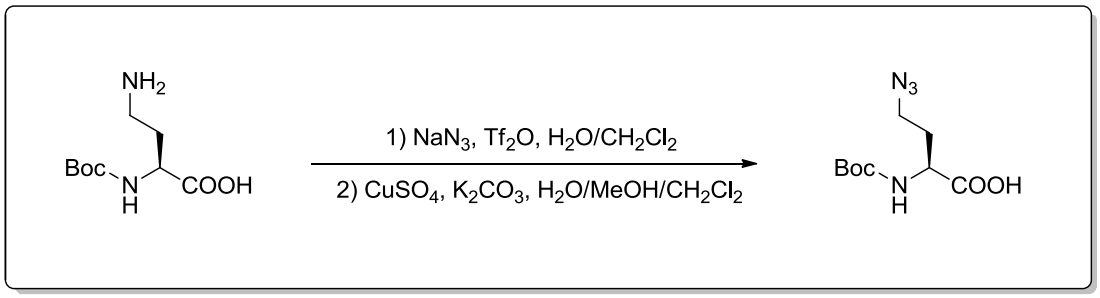

Sodium azide (9.8 g, 150 mmol) was dissolved in a mixture of water (22 mL) and dichloromethane (39 mL). The contents were cooled in an ice bath, and triflic anhydride (5.1 mL) was added via syringe over 5 minutes. The contents were allowed to stir for 30 minutes, after which the layers were separated. The aqueous layer was extracted using dichloromethane (2 × 50 mL). The organic fractions were pooled, and washed twice with 5% aq. sodium carbonate (30 mL). The triflyl azide containing organic layer was then added to a solution of *N*-tert-butoxycarbonyl-(S)-2,4-diaminobutanoic acid (3.1 g, 14.2 mmol) in water (39 mL) and methanol (90 mL). To this, potassium carbonate (3.2 g) and copper sulphate pentahydrate (38.4 mg) were added. Stirring was continued for 18 h, after which the organic fraction was evaporated in vacuo. The aqueous portion was extracted with dichloromethane (2×50 mL), diluted with water, then acidified to pH 2.0 using 1.0 N hydrochloric acid. The acidified aqueous phase was then extracted with dichloromethane (3 × 50 mL). The organic phase was then washed with brine (2 × 80 mL), dried with magnesium sulphate, filtered, and evaporated. The product was obtained as orange oil (3.2 g, 92%). IR (ν_{max}, film): 3319, 2980, 2935, 2100, 1690, 1513, 1455, 1399, 1369, 1236, 1189, 1154, 1093, 1057, 1029, 940, 853. ^{1}H NMR (400 MHz, $CDCl_3$) δ: 5.26 (br d, *J* = 8.8 Hz, 1H, N*H*), 4.41 (m, 1H, C*H*), 3.46 (t, *J* = 6.7 Hz, 2H, N_3CH_2), 2.11 (m, 1H, C*H*$_2$), 1.98 (m, 1H, C*H*$_2$), 1.46 (s, 9H, C(C*H*$_3$)$_3$).LRMS (ESI) Calculated: [M-H] $C_9H_{16}N_4O_4$ (m/z) : 243, Obtained: $[M-H]^-$: 243.08, $[2M-H]^-$: 487.16

Step 3: Deprotection of Boc:

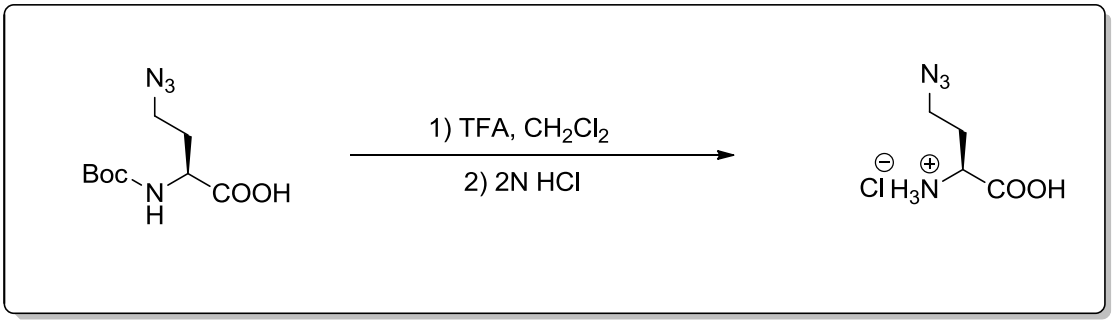

N-tert-Butoxycarbonyl-(*S*)-azidohomoalanine (3.2 g, 13.11 mmol) was dissolved in dichloromethane (55 mL), to which trifluoroacetic acid (29 mL) was added. The contents were stirred at room temperature for 3 hours. The solvent was then evaporated, and the oily residue redissolved in 2.0 N hydrochloric acid (45 mL). Further evaporation yielded solid L-azidohomoalanine (1.13 g, 61 %). IR (v_{max}, film): 3368, 3036, 2978, 2926, 2103, 1677, 1589, 1489, 1351, 1333, 1265, 1204, 1101, 854, 771. ^{1}H NMR (400 MHz, D_2O) δ: 3.99 (t, *J* = 6.32, 1H, CαH), 3.48 (t, *J* = 6.4, 2H, CH_2N_3), 2.07 (m, 2H, $C\beta H_2$). ^{13}C (400 MHz, D_2O) δ: 57.8 (Cα), 47.6 (CH_2N_3), 29.6 (Cβ). LRMS (ESI) Calculated: [M+H] $C_4H_8N_4O_2$ (m/z): 144, Obtained: $[M+H]^+$: 145.08, $[M+HCl-H]^-$: 179.06, $[2M-H]^-$: 287.11, Melting pt. 180.6 ˚C, $[\alpha]^{20}_D$ = +6.60º (c = 0.50, H_2O).

Synthesis of *tris*-triazolyl Ligand.

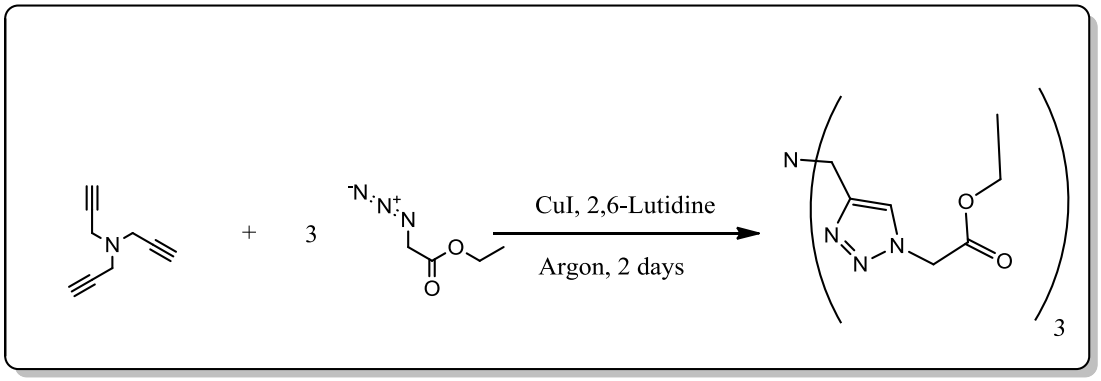

The tris-triazole ligand, triethyl 2,2',2''-(4,4',4''-nitrilotris(methylene)tris(1H-1,2,3-triazole-4,1-diyl))triacetate, was prepared following minor modification of the methodology described by Zhou and Farni.[27] Sodium azide (2.31 g, 35.5 mmol) was suspended in 5 mL dimethylformamide, to which ethylchloroacetate (3 mL, 28.0 mmol) was added dropwise at room temperature, and stirred for 24 hours. The solution was then diluted with diethyl ether (150 mL) and washed with water (3 × 30 mL). The organic layer was then dried with sodium sulphate, filtered, and concentrated to 10 mL. This was then added to a solution of containing

tripropargylamine (0.65 g, 3.8 mmol) in acetonitrile (5 mL), flushed with argon. The solution was cooled in an ice bath, and 2, 6-Lutidine (0.6 mL) and copper (I) iodide (20 mg) were added under a stream of argon. After 1 hour, the ice bath was removed, and stirring was continued for 2 days under argon. The solvent was then evaporated, and the residue purified by column chromatography (1:10 methanol: ethyl acetate) to give the product as a white solid (1.95 g, 98.7 %). IR (v_{max}, film): 3141, 2985, 2947, 2906, 2830, 1745, 1559, 1465, 1450, 1413, 1398, 1379, 1351, 1329, 1309, 1261, 1222, 1181, 1143, 1128, 1107, 1080, 1047, 1024, 971, 947, 931, 879, 839, 805. ^{1}H NMR (D_2O, 400 MHz) δ: 7.94 (s, 3H, triazole), 5.17 (s, 6H, C*H*$_2$COOEt), 4.26 (q, 6H, J = 7.17 Hz, COOC*H*$_2$CH3), 3.87 (s, 6H, NC*H*$_2$-triazole), 1.29 (t, 9H, J = 7.17 Hz, COOCH$_2$C*H*$_3$). LRMS (ESI) Calculated: [M+H] $C_{21}H_{32}N_{10}O_6$ (m/z) : 519.2, Obtained: $[M+Na]^+$: 541.2, Melting pt. 106.2 ˚C

Cell viability assay by flow cytometry

Jurkat T cells or primary human T-lymphocytes were starved and labelled with 'heavy' arginine and 'heavy' lysine amino acids as described in the Methods section of the paper. Different concentrations of azidohomoalanine (AHA) (1 mM, 4 mM) and as a control, L-methionine (Met) (1 mM, 4 mM), were used. Primary human T-lymphocytes were treated in the presence or absence of PMA (100 nM) and Ionomycin (1.4 µM). Determination of apoptotic cells under these conditions was performed by phosphatidylserine staining on the cell surface using allophycocyanin (APC) conjugated Annexin V. For each condition, 0.5×10^6 cells were harvested after 2 and 4 hours of amino acid incorporation in a 96 well microtiter plate and washed once with PBS. After resuspension in 100 µL Annexin-binding buffer (Invitrogen) containing APC-conjugated Annexin V (Beckman Coulter), cells were incubated for 15 minutes at room temperature in the dark. For flow cytometric analysis cells were centrifuged, resupended in 300 µL Annexin-binding buffer and transferred to flow cytometry tubes. Annexin V positive cells and cell morphology were analyzed immediately by FACSCalibur™ flow cytometer (BD Bioscience) and FlowJo software.

Biosynthetic labelling by ^{35}S-Cysteine pulse and pulse-chase

Jurkat T cells were centrifuged and washed once in warm RPMI without L-methionine and L-cystine (R7513 SIGMA), supplemented with 10 % dialyzed FBS (Gibco) and L-glutamine (PAA). After starvation of methionine and cysteine for 1 hour at 37 °C in the same media at a cell density of 1×10^6/ml, equal numbers of cells were centrifuged in four sets. Two sets of cells (2×10^6/ml) were placed in fresh, warm RPMI starvation media (see above) containing L-Azidohomoalanine (AHA) at a final

concentration of 1 mM or 4 mM, while the other sets of cells were placed in media containing 0.1 mM L-methionine or without methionine as a control. The media for all sets was simultaneously supplemented with 10 nM (10 µCi/ ml) L-[^{35}S]-cysteine (PerkinElmer) and 5 µM L-cystine (from RPMI SILAC media, Dundee Cell Products). A sample of 2×10^6 cells of each replicate per condition was taken immediately as a reference for 0 hours of "pulse". The "pulse" was performed at 37 °C and samples (2×10^6) for each replicate per condition were harvested after 2 and 4 hours. Cell lysates for protein precipitation were prepared as follows: cells were centrifuged and washed two times with 1 mL cold RPMI-1640 (PAA) supplemented with 10 % FBS (HyClone Thermo) and two times with 1.2 mL cold 50 mM iodoacetamide in PBS. Cell pellets were lysed for 10 minutes in 25 µL 1 % SDS in PBS containing protease and phosphatase inhibitors (Complete EDTA-free, Roche, 2mM sodium pervanadate) and benzonase (100 Units). The samples were then centrifuged at 20,000g for 10 minutes and the supernatant was stored on ice. All replicates for each time point were spotted together on a Watman filterpaper, which was then incubated three times for 5 minutes with 5 % trichloroacetic acid for protein precipitation. After rinsing the filter paper with 70 % ethanol and 100 % acetone, each sample was placed in 4 ml scintillation fluid (Optiphase Supermix, Perkin Elmer) and counted in a scintillation counter for 3 minutes (Packard TriCarb 2900TRLiquid Scintilliation Analyser, GMI).

For the analysis of protein degradation, Jurkat T cell were washed and starved as described for the pulse experiment. After starvation, two sets of cells (2×10^6/ml) were placed in fresh, warm RPMI starvation media (see above) containing L-azidohomoalanine (AHA) at a final concentration of 1 mM while the other set was placed in media containing 0.1 mM L-methionine. The media for both sets was simultaneously supplemented with 32.4 nM (30 µCi/ml) L-[^{35}S]-cysteine (PerkinElmer) and 16.2 nM L-cystine (RPMI SILAC media, DundeeCell). The "pulse" was performed for 15 minutes at 37 °C. Cells were then centrifuged for 5 minutes and washed once with RPMI-1610 media (PAA) lacking L-[^{35}S]-cysteine and supplemented with 10 % FBS (HyClone Thermo). The "chase" of L-[^{35}S]-cysteine was performed by resuspending the cells in fresh warm RPMI-1640 media at a density of 2×10^6/ml. A sample of 2×10^6 cells for each replicate per condition was taken immediately as a reference before chasing of [^{35}S]-cysteine took place. For each replicate, 2×10^6 cells were harvested after 1, 2 and 4 hours "chase". Preparation of cell lysates, protein precipitation and measurement of radioactivity was performed as described above.